



GIS-based multielement source analysis of dustfall in Beijing: A study of 40 major and trace elements



Nana Luo ^{a, b}, Li An ^b, Atsushi Nara ^b, Xing Yan ^{a, c}, Wenji Zhao ^{a, *}

^a College of Resource Environment and Tourism, Capital Normal University, Beijing, China

^b Department of Geography, San Diego State University, 5500 Campanile Dr., San Diego, CA, 92182-4493, USA

^c Department of Land Surveying and Geo-Informatics, The Hong Kong Polytechnic University, Hong Kong, China

H I G H L I G H T S

- 40 major and trace elements were investigated from the dustfall in Beijing.
- Local or nearby cities of pollution sources were identified by GIS.
- Source apportionment was examined and modified using land use data and terrain information.

A R T I C L E I N F O

Article history:

Received 22 December 2015

Received in revised form

21 February 2016

Accepted 23 February 2016

Available online xxx

Handling editor: Ralf Ebinghaus

Keywords:

Dust

Trace elements

Backward-trajectory model

GIS

A B S T R A C T

Dust, as an important carrier of inorganic and organic pollutants, daily exposes to human without any protection. It affects our health adversely, especially its chemical elements and ions. In this research, we investigated the chemical characteristics of dustfall in Beijing, specifically in terms of 40 major and trace elements, and presented semi-quantitative evaluations of the relative local and remote contributions. In total, 58 samples were collected in Beijing and nearby cities during 2013–2014 “the winter heating period”. Using multiple statistical methods and GIS techniques, we obtained the relative similarities among certain elements and identified their pollution sources (from local or nearby cities). And more interestingly, the relative contributions of nearby cities can be calculated by the Hysplit4 backward-trajectory model. In addition, the correlation analysis for the 40 elements in dust and soil indicated that traffic restricted interchange between them; the city center, with the heaviest traffic, had the most significant influence. Finally, the resulting source apportionment was examined and modified using land use data and terrain information. We hope it can provide a strong basis for the environmental protection and risk assessment.

© 2016 Elsevier Ltd. All rights reserved.

1. Introduction

Urban dustfall is generally regarded as an accumulation of suspended particulate matter, derived from several sources, including natural processes and intensive human activities. It is a mixture of organic and inorganic particles floating under atmospheric transportation or transferred by anthropogenic contamination. As an important carrier of air pollutants, the deposited dust can pose serious risks to the environment (Shparyk and Parpan, 2004). In particular, its chemical components, such as major and trace elements, adversely affect human health (Zencak et al., 2007;

Jeong et al., 2013). For example, some elements can increase the rates of carcinogenic and respiratory diseases, cause deterioration of lung function, and raise the need for emergency treatment (Green and Armstrong, 2003; Qian et al., 2007). Therefore, identifying the sources of airborne dust-carried elements is of vital importance to human daily life. In addition, elemental analysis and source apportionment of dustfall can generate highly useful information on atmospheric pollution assessment and can be used as a powerful tool for decision making in environmental protection.

Recently many studies have found that elemental components extracted from dust can come from Earth's crust or surface soil by natural processes, vehicle exhausts, industrial activities, and residential heating (Celo et al., 2015; Jiang et al., 2015a,b; Tan et al., 2014). And in a long-term perspective, they can be generated from local man-made contributions and also be transported from

* Corresponding author.

E-mail address: zhwenji1215@163.com (W. Zhao).

nearby cities (Olmez and Gordon, 1985; Taylor and McLennan, 1995; Kitto et al., 1992). Due to the complexity of the elements carried by dustfall, it is a challenge to determine the local and remote emissions and to qualify the relative contributions.

In terms of local source appointment, enrichment factor (EF) has been widely proved to be a popular means to identify human intervention in global element cycles (Lin et al., 2015; Tian et al., 2014). The EF value for a certain element in materials can indicate whether the investigated element is enriched (Censi et al., 2011). However, according to Reimann's study, there are several serious flaws in calculation of EFs (Reimann and Caritat, 2000). The values reflect only the relative solubility of different elements and cannot differentiate between human and natural sources, because only the weathering and winnowing of fines are considered and the impact of biogeochemical processes is neglected. As a reference, the Earth's crust at each site varies largely, so a global average value used in most relevant studies cannot be available. Regardless of the theoretical deficiencies of EFs, the conclusions drawn by most studies are limited to be only human activities versus geogenic sources. This is far from ideal, especially for big cities due to their complex and sophisticated underlying state; moreover, rapid urbanization and industrialization have brought multiple new pollutants, overriding the original EFs. Nowadays a given source can release several contaminants or elements, so the concept of EFs – with one specific element under investigation – sometimes is invalid.

Accordingly, a multielement-based analysis that considers the associations between elements, classifies them into certain groups, and identifies the source of each group separately is proposed in this study. It can be realized by using principal component analysis (PCA), cluster analysis (CA), and correlation analysis (CO). Specifically, CA has shown an excellent performance in categorizing complex datasets based on relevance. For example Beddows et al. (2014) presented a cluster analysis of particle number size distributions and successfully used air-mass back-trajectories to examine the evolution of aerosol size distributions in real time. Overall, CA simplifies the dataset greatly and allows an easy intercomparison between clusters. Moreover, the multielement analysis is further extended by PCA. A great advantage of PCA is not just the potential use of dimensionality reduction, but also the qualified results for the following comparisons (Zhang et al., 2012). Thus, this study focuses on not a single element, but a set of elements with the closest connection.

As for remote source identification, many studies have been conducted by air-mass backward-trajectory (Chen et al., 2014a,b; Zhang et al., 2015). This technique is commonly used to compare different sites over long periods and to link geographical source to emission source (Cape et al., 2000; Wang et al., 2014). Recently the potential use of backward trajectories for modeling the transport and dispersion of tracers has been discussed and improved. For example, simulations with high temporary and spatial resolution using a mesoscale meteorological model have been used to improve the accuracy of trajectory calculations over a region with complex topography (Ashbaugh et al., 1985). A residential time analysis has been developed for back trajectories, known as the potential source contribution functions (Robinson et al., 2011). In most studies there are total two different methods applied to interpret the trajectories: comparing the periods classified by a cluster analysis of trajectories, and inspecting the mean values of historical trajectories (Pinxteren et al., 2010). Due to the high uncertainty of a single trajectory, in practice, large numbers of trajectories are usually used to identify the sources (Kleiman et al., 2006). However, it is a challenge to differentiate an oriented pollution source from the total emission and to quantify the relative contributions. Thus, the concept of cluster-weighted probability can be used to calculate it (Gao et al., 2014).

In addition, many studies have included dustfall component analysis (Tang et al., 2013; Yang et al., 2015; Cao et al., 2011; Shaltout et al., 2013). Nevertheless, there has been little research involving a whole distribution (Zhang et al., 2013; Biegalski and Hopke, 2004). Furthermore, part of these studies has involved only a few sites or limited elements, although sampling was performed over a long period, which is obviously ineffective. Because research on atmospheric pollution itself is a large-scale issue, single-point experiments cannot provide sufficient information for relevant policy-makers. In this paper we overcame the limitations of single-point sampling and limit-element investigation in atmospheric studies by analyzing 40 elements distributed in the whole Beijing area, including industrial metal elements, actinide and lanthanide elements. Their sources were identified by a series of statistical methods. Then the final result was further extended by using backward trajectories, land use, and digital elevation model (DEM). Especially DEM was used to improve the source analysis by comparing the elemental difference between high and low terrains.

To sum up, in this study we use ArcGIS mapping technique to visualize the result. And most importantly the original data is point-level. Thus, we apply ArcGIS interpolation technique to obtain a whole distribution. Additionally, the concept of spatial analysis in GIS is introduced to extend the research. On the basis of the statistical result, we calculate the spatial variation along a trajectory.

2. Method

2.1. Area

The study site was located in Beijing, the economic, political, and cultural center of China (39.4° to 41.6°N, 115.7° to 117.4°E). This region enjoys a climate typical of a semi-humid continental monsoon: hot and rainy in the summer and cold and dry in the winter. In this study, the whole Beijing metropolitan area, including the four suburban districts Changping, Shunyi, Haidian, and Chaoyang, was selected to investigate spatial differences in the distributions of 40 elements (See Fig. S1, Supplementary data). In addition, four cities Baoding, Langfang, Cangzhou, and Shijiazhuang were chosen as reference sites. These sites were selected due to the terrain of the city: Beijing is embraced by the mountains at the north, west and northeast sides. The purpose of these reference sites was to illustrate the impact of surrounding areas on Beijing and to summarize the immigration paths of given elements. In total, 47 and 11 plots were selected in Beijing and at the reference sites, respectively. At the former, we collected dust and soil examples and at the latter, only dust (Fig. 1).

2.2. Sampling and elemental analysis

Dustfall accumulated from Nov. 15, 2013 to Mar. 15, 2014: namely, “the winter heating period”. The collection containers were 10 × 10 × 10 cm³ plastic bottles hung on telephone poles in Beijing and other surrounding cities. In total, we used more than 100 bottles, but only 60 bottles were recovered. To get a reasonable distribution of the elements in a large scale, the sampling sites were chosen randomly. Moreover, this sampling was not limited at a single site, but distributed in the whole area, which could better reflect the elements in a large scale and get more useful compared to the single-point sampling. When these bottles were collected, the soil was sampled from the surface layer (0–5 cm), placed into clear polyethylene bags and then brought to the laboratory for further study. Next, 40 mg of each dust sample with a mixture of 2 mL HNO₃ and 0.6 mL HF were transferred into Teflon vessels and heated to 150 °C for 24 h. After cooling, 0.5 mL HClO₄ was added,

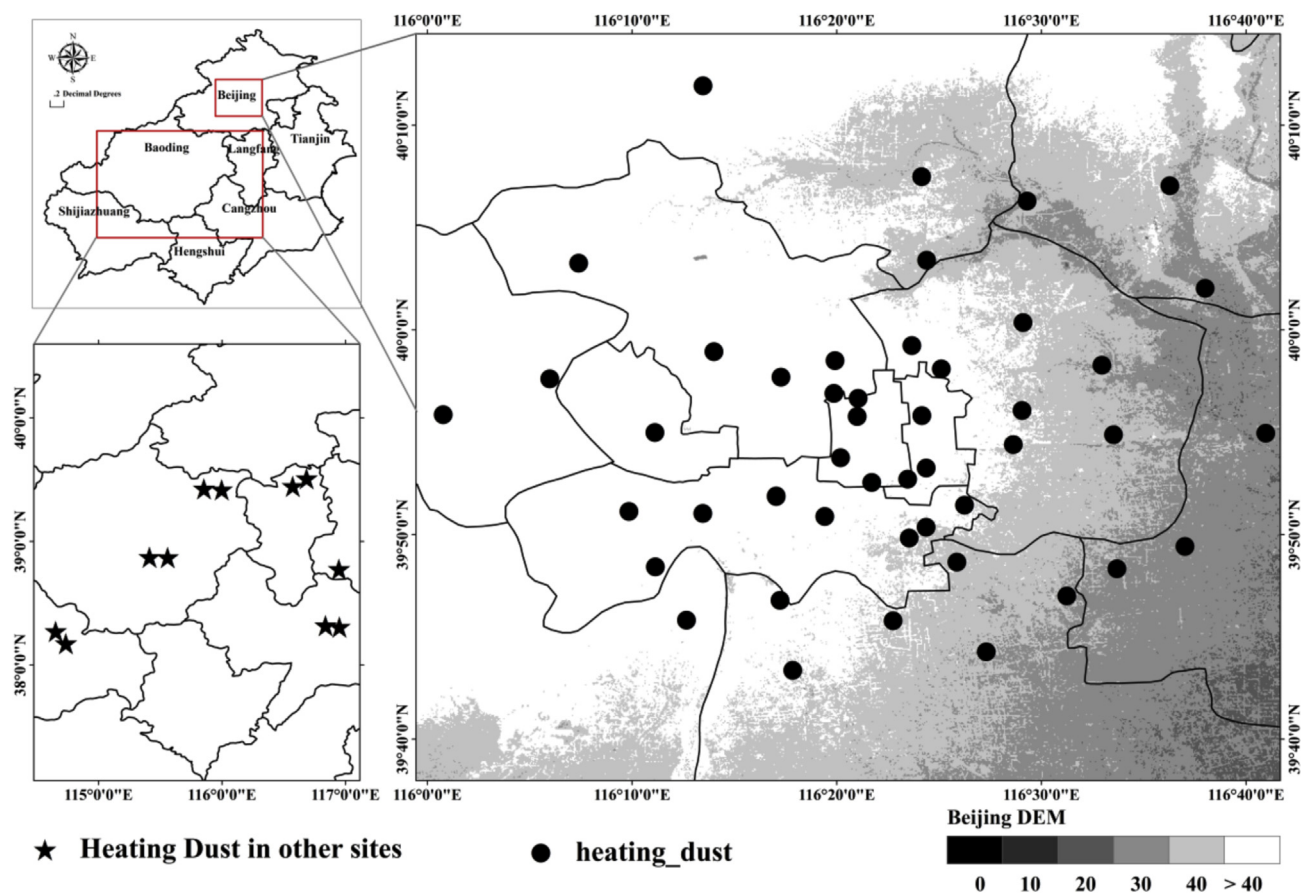


Fig. 1. Map of sampling sites (From Fig. 1 we can see that the whole Beijing has a lower trend in the eastern and southern part, this fact will be used to explain the spatial distribution of major and trace elements collected from Beijing airborne particles. Right figure is Beijing main district where 47 samples were collected for dust and soil (except lost). Left figure is Beijing surrounding cities where 11 samples were obtained only for dust (except lost). The reason we only picked dust in other areas is that airborne dustfall can be easily moved by air and thus can be better used to study the immigration path of air major and trace elements.).

and heated uncapped on an electrical hot plate (150 °C) until dry. Samples were re-dissolved with 1 mL pure water and 1 mL HNO_3 for 12 h before the solution was transferred to a clean flask and diluted with pure water to 40 mL. Finally, the concentrations of Li, Be, Ga, Pr, Nd, Sm, Eu, Tb, Ho, Yb, Lu, Er, Th, U, Hf, V, Gd, Rb, Cs, Nb, Ta, Sc, Sr, La, Ce, Cd, Zr, Y, Co, Cu, Bi, Mo, W, Ni, Cr, Dy, Ba, Zn, and Pb were determined by ICP-MS. For quality assurance and control (QA/QC), repeated and reference samples (GBW07315, GBW07316, BCR-2, and BHVO-2) were processed again. The relative standard deviation was below 6.5%; the relative error was below 5%.

2.3. Statistical methods

Standard statistical measures (mean, standard deviation (SD), coefficient of variation (CV), minimum (Min), maximum (Max)) were used to describe the elemental concentrations of dustfall. These variables are essential to quantify differences between sampling sites in the accumulation of elements. Then, cluster analysis and correlation analysis were carried out to identify the approximate pollution sources for Beijing airborne elements (from local, outside, or both): the former was conducted among sampling sites, including those in and outside Beijing. Thus, we were able to determine whether some of the elements came from the nearby area. Correlation analysis provided a technique to understand the relationship between dustfall and soil, and we could decide whether local pollutants contributed to the elements. Finally, principal component analysis was used to reduce the dimensions of

the data set and to quantify the contents in the same clusters. Before that, a cluster analysis between elements, different from the first CA, was performed and elements were classified into certain groups. Then, PCA was applied to each cluster. Each group had a PCA score that indicated the level of investigated elements, which was used for further analysis.

2.4. Back trajectory and underlying analysis

To understand the remote and local sources of elements in Beijing dustfall, the HYSPLIT_4 model (Hybrid Single-Particle Lagrangian Integrated Trajectory, Ver. 4.9), was used to compute 72-h backward trajectories every 6 h during the sampling period (Gaita et al., 2014; Wang et al., 2009). The site was located at 40°N, 116°E and the relative height was 10 m. Meteorological data were obtained from the Air Resources Laboratory website in GDAS format at half-degree spatial resolution. The trajectories were re-input to the HYSPLIT_4 model for a cluster analysis and certain main trajectories were obtained. As mentioned above, PCA scores for 47 sites were interpolated to an overall scale by a Kriging method. They were then assigned to each mean trajectory to quantify the element immigration. The detailed procedure is shown as Equation (1): the PCA change along a trajectory was calculated and combined with the contribution ratio of the trajectory the total contribution of each direction was computed. Additionally, integrated with the statistical results of elements, underlying surface and profile analyses were used to analyze the

local sources. The Land Cover and Land use data was obtained from the project of “Beijing Land Cover and Land Use Monitoring”. The spatial resolution is 30 m.

$$IA = (C_{\text{ending}} - C_{\text{starting}}) * CR_{\text{trajectory}} \quad (1)$$

where IA is the total contribution of a certain trajectory, C_{starting} and C_{ending} are the PCA scores of the starting and ending points along the trajectory, and $CR_{\text{trajectory}}$ is the contribution ratio of the trajectory.

3. Results and discussion

3.1. Major and trace element concentrations of dustfall

Statistical information for the elements (See Table S1, Supplementary data) during the last winter heating period is presented (See Table S2, Supplementary data). To assess the elements, the mean concentrations and variation coefficients were computed. For soil, the concentrations of Ba, Sr, Zn, and Zr were highest, while Ba, Sr, Zn, Cu, Cr, Zr, and Pb were highest for dust. Although dust and soil showed similar trends for certain elements, the concentrations were significantly different. For example, Ba, Sr, Zn, and Zr ranked first for soil and dust: mean Ba varied from 634.30 to 1302.00 $\mu\text{g/g}$, Sr varied from 300.20 to 706.00 $\mu\text{g/g}$, Zn varied from 133.12 to 399.60 $\mu\text{g/g}$, Zr varied from 131.64 to 138.10 $\mu\text{g/g}$, Cu varied from 51.52 to 205.20 $\mu\text{g/g}$, and Pb varied from 35.24 to 101.05 $\mu\text{g/g}$, respectively for soil and dust.

In addition, the largest difference between dust and soil was observed in the variation coefficient. In soil, Bi, Cu, Zn, Cr, and Pb showed the largest variability, while in dust La, Ce, Sr, Cr, and Ba varied most. Specifically, Bi varied from 0.15 to 5.07 $\mu\text{g/g}$, Cu varied from 19.62 to 306.00 $\mu\text{g/g}$, Zn varied from 54.17 to 478.74 $\mu\text{g/g}$, Cr varied from 50.68 to 192.76 $\mu\text{g/g}$, and Pb varied from 19.82 to 88.05 $\mu\text{g/g}$ in the soil group, whereas La varied from 18.8 to 686.90 $\mu\text{g/g}$, Ce varied from 37.60 to 1417.20 $\mu\text{g/g}$, Sr varied from 220 $\mu\text{g/g}$ to 9221.00 $\mu\text{g/g}$, Cr varied from 85.90 to 1242.10 $\mu\text{g/g}$, and Ba varied from 557.00 to 8565.00 $\mu\text{g/g}$ in the dust. Thus, these results suggest that the pollution sources for dustfall and soil in Beijing vary significantly. Some sites had extremely high concentrations of certain elements, such as Cu in TianTanBeiLu soil and La in WanShouPark dust, showing that some non-natural pollutants change the balance of dust and soil.

A comparison of elements among sites can be made using standard statistical variables; however, it is too simple to analyze the element distributions. The concentrations of the elements at different sites are described (See Fig. S2, Supplementary data). Extremely high values existed, such as Cu at DongSiBeiDajie, Y at ZhouJiaGangQiao, Zr at SanJiaDianXiKou, Nb and Ta at TianTanBeiLu, Mo and W at QianMenDongDajie, Ba at JiMenQiaoNan, Pr, Nd and Eu at YongDingMenNeiDajie, Dy at XiangShanNanLu, and Bi at FengBeiQiao. In total, about 26 elements were significantly high at WanShouPark, which may be related to its surroundings or the extraction procedure. Another experiment was repeated at the same place and the results were the same. Also, in field surveying, the sample for WanShouPark was collected near a road; its north and southeast areas included two large parking sites, and its southwest area included a construction site. Compared with other locations, Wan Shou Park had a more sophisticated road network and man-made pollution sources.

3.2. Source identification of Beijing airborne elements

Cluster analysis is a common statistical method in component

analysis in environmental studies. The data are first standardized, a Euclidean distance for similarity between variables is calculated, and then a hierarchical cluster model is built with the standardized data set. Previous studies usually calculated a Euclidean distance for similarities among elements (Beddows et al., 2009). However, in this study, we performed a cluster analysis using the element concentrations to calculate a Euclidean distance for similarities among sampling sites. This was helpful to identify whether airborne elements in Beijing had a connection with nearby cities. Ward's method of ANOVA uses the sum of squares between two clusters to add up all the variables. The sampling sites can be divided into four groups (See Fig. S3, Supplementary data): (1) WanShouPark and WanPingGuCheng; (2) JiMenQiaoNan; (3) SanJiaDianXiKou, YingHuaQiaoDongJie, BaiJiaoBeiLu, and SiHuiQiao; and (4) other, including 35 Beijing sites and 11 reference sites (outside Beijing). From these results, it is evident that 84% of the sampling sites in Beijing and all sites in surrounding cities were divided into the same group. This indicates that Beijing and nearby cities have strongly interrelated pollution mechanisms for airborne elements, and that local pollutants affect the element concentrations more in the other three groups than in group 4.

To some extent, the correlation results for the dustfall and soil in terms of element concentrations reflect a degree of similarity between them. They may have similar origins or may be caused by different pollutants. Thus, a correlation coefficient of dustfall and soil was calculated to measure the relationship and interpolated to a whole distribution by a Kriging method. Fig. 2 shows the correlation results for dustfall and soil by element. The correlation coefficient was found to be in the range 0.50–0.99: it was around 0.5 in the middle of Beijing and exceeded 0.88 in Beijing's upper parts. That is, the middle area had a lower correlation than other parts, which may be related to the complex road network and heavy traffic volume. Heavy traffic in the middle of Beijing probably causes vortex and convection motions that create an extremely unstable environment, forcing airborne particles to move. For example, the area within the Second Ring Road in Beijing showed the lowest correlation (almost 0.5) and this area usually has the heaviest traffic. Obviously, local pollutants contribute greatly to the elemental concentrations of Beijing dustfall.

3.3. Cluster and principal component analysis

To find local and remote sources for the elements, CA between 40 elements and PCA for each group were conducted. CA categorizes elements into groups based on their levels of correlation, and PCA quantifies a specific cluster to measure the levels of specific elements uniformly. Variables in the same group have the closest connection and those in different groups share a weak correlation. Thus, variables in the same basic structure may have similar sources and their combination calculated by PCA is decisive in identifying pollution levels. The results of the cluster analysis among elements are illustrated (See Fig. S4, Supplementary data), which differed from the first CA among sampling sites. In total, the 40 elements were grouped into 10 clusters (C1, C2, C3, C4, C5, C6, C7, C8, C9, and C10): (1) Li, Be, Ga, Pr, Nd, Sm, Eu, Tb, Ho, Yb, Lu, Er, Th, U, Hf, V, Gd, Rb, Cs, Nb, Ta, Sc, Sr, La, Ce, Cd, Zr, Y, and Co, (2) Cu and Bi, (3) Mo, (4) W, (5) Ni, (6) Cr, (7) Dy, (8) Ba, (9) Zn, and (10) Pb. Similarities for the first and second clusters reached 82.84% and 81.35%, respectively; the others were less than 80%. Obviously, the elements in C2 to C10 may cause more serious pollution than those in C1, which may come almost entirely from soil. Additionally, Cu, W, Ni, Cr, Ba, Zn, and Pb are typical industrial metals and were put into separate groups. Industrialization and urbanization in Beijing definitely have non-negligible influences on these elements.

Subsequently, PCA was used for each cluster, except those

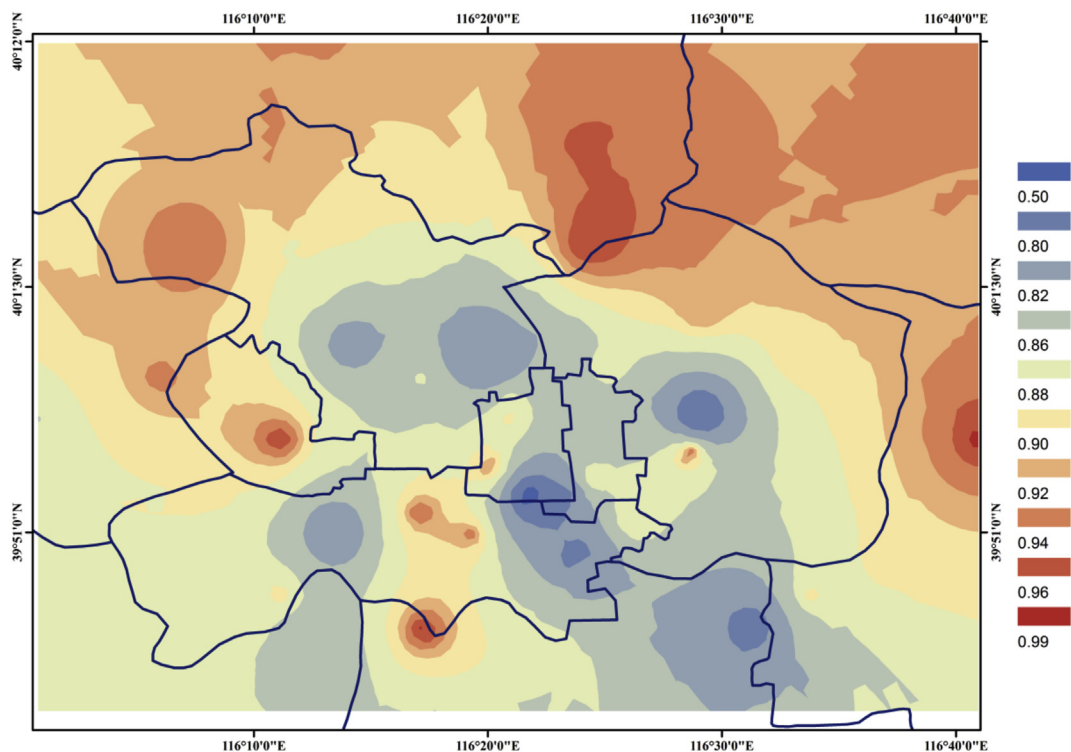


Fig. 2. The spatial distribution of Pearson's correlation coefficient of dustfall and soil samples collected from Beijing main area (Pearson's correlation coefficient of dustfall and soil is computed by using the concentrations of 40 major and trace elements at each sampling site. Then interpolation is conducted by Kriging method and a whole Pearson's distribution is obtained. The Pearson's coefficient varies from 0.5 to 0.99 and from its spatial variation pollution sources for these 40 major and trace elements are roughly determined).

involving only one element. With linear transformation and matrix orthogonalization, the components were obtained and decreasingly sorted by their loadings; those with an accumulation proportion above 80% were selected as the principal components. Here, the values were 81% and 82% for C1 and C2, respectively (See Table S3, Supplementary data). C1 had three principal components: C1-1, C1-2, and C1-3, and C2 had one (C2-1). For C3 to C10, we used the standardized element concentrations instead. The principal components for C1 and C2, loading values for each element, and PCA scores for each site are presented (See Fig. S5, Supplementary data). Detailed information about the sampling sites is described (See Table S4, Supplementary data), and the PCA scores for C1 to C10 are reported (See Table S5, Supplementary data). C1-1 mainly included Sm, Ho, Tb, Er, Yb, La, Lu, Th, Eu, Ce, Nd, Pr, Gd and U, C1-2 contained Cd, Co, Cs, Li and Ga, and C1-3 covered Ta. However, C2 consisted only of Cu and Bi. Specifically, LiShuiQiao had the highest score for C1-1, and YongChang ZhongLu ranked first for C1-2, while ZhiChunLu and TianTanBeiLu were at the bottom. This indicates that LiShuiQiao and YongChangZhongLu had the total highest levels of Sm, Ho, Tb, Er, Yb, La, Lu, Th, Eu, Ce, Nd, Pr, Gd, U, Cd, Co, Cs, Li, and Ga, while ZhiChunLu and TianTanBeiLu had the lowest. In the same way, FengBeiQiao had the highest concentrations of Cu and Bi, whereas YongDingMenNeiDajie had the lowest. The aim of the PCA analysis was to quantify the relevant elements in total, and to further compare their contents.

3.4. Backward trajectory analysis

After the pollution sources of the elements in Beijing dust had been determined to be local pollutants and from nearby cities, detailed sources and immigration paths needed to be identified. Fig. 3 describes the backward trajectories ending at Beijing and cluster analysis of the trajectories during the sampling period. The

backward trajectories were obtained every 72 h and the end points for each trajectory were calculated for each 6-h period. There were, in total, 142 trajectories computed with the HYSPLIT_4 model, shown at the bottom right of Fig. 3. To determine the main directions of the air masses, a cluster analysis for 142 backward trajectories was performed by special runs of the HYSPLIT_4 model and four clusters were acquired, as shown in the top right of Fig. 3. Generally, four categories of air masses were identified: (1) SE – air masses that had originated in the southeast of the continental area and passed through Beijing, Tianjin, and Hebei; (2) N – air masses that had originated in the north of Mongolia and passed through Mongolia, Inner Mongolia, and Zhangjiakou; (3) NW – air masses that had originated in Kyzy and passed through Mongolia and Inner Mongolia, and (4) W – air masses that had originated in Biysk and passed through Mongolia and Inner Mongolia. The contribution ratios were 14.4%, 26.9%, 28.4%, and 30.2%, respectively. Thus, during the sampling period, Beijing was generally dominated by air masses from the W, NW and N, with fewer from the SE.

3.5. Detailed local and remote source appointment

PCA scores obtained from the 47 sites were interpolated to a whole scale by Ordinary Kriging Model which has been proved to have a good performance in urban-scale study with limited sampling points (Kim et al., 2014). In order to identify the best semi-variogram we compared different regression models and evaluated various combinations of nearest neighbor, lag size, and number of lags. Finally we selected ordinary Kriging with Circular model for the interpolation. The cross-validation of multiple regression models in Ordinary Kriging is shown in Table S6, Supplementary data. The interpolation results for C1 to C10 (See Fig. S6, Supplementary data) are described. C1-1, C1-2, and C1-3 represent the three principal components for C1, and the high zones were

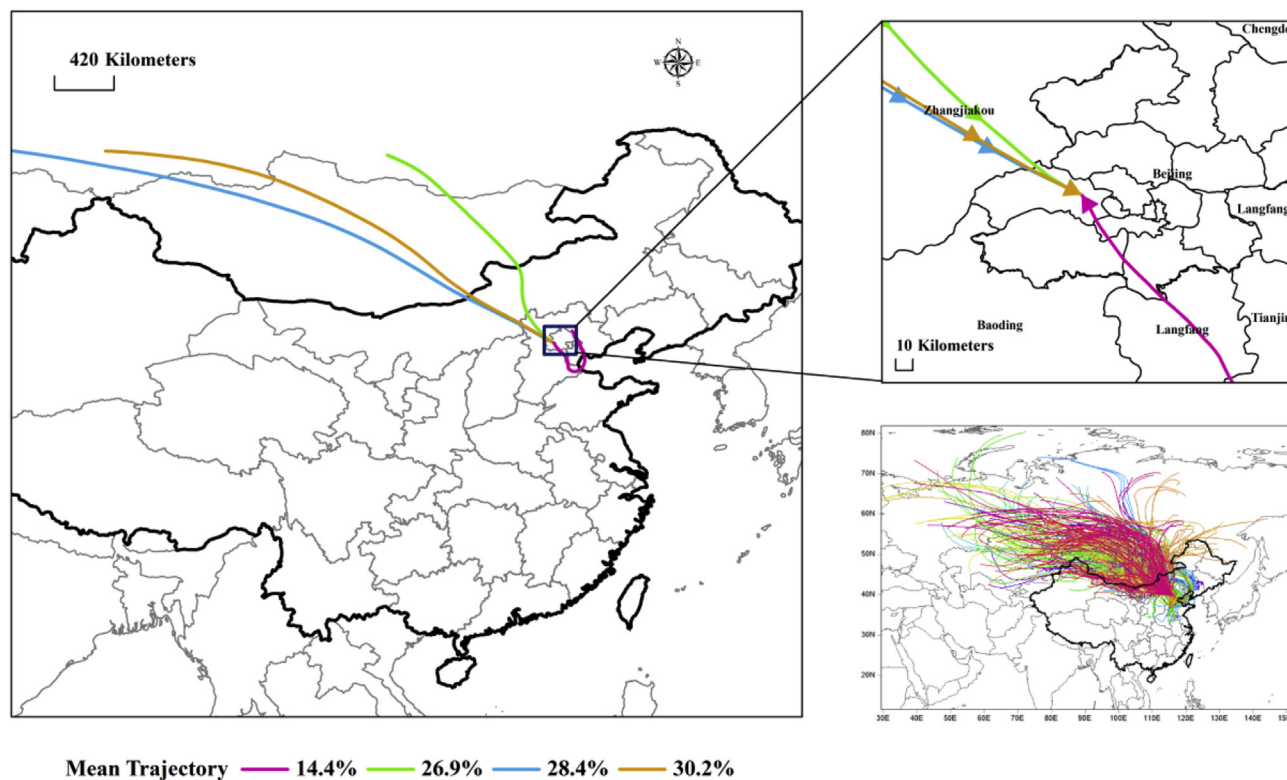


Fig. 3. The backward trajectories of air masses arriving at Beijing from Nov. 15 in 2013 to Mar. 15 in 2014 (142 trajectories are calculated and four clustered trajectories are obtained, of which the contribution ratios are, respectively, 14.4%, 26.9%, 28.4% and 30.2%). The concentrations of 40 major and trace elements will be assigned to each mean trajectory by Kriging interpolation and the corresponding immigration amount will be identified.)

Beijing's two sides and center, the city's two flanks, and the southwest of the city. Sm, Ho, Tb, Er, Yb, La, Lu, Th, Eu, Ce, Nd, Pr, Gd, and U correspond to C1-1; Cd, Co, Cs, Li, and Ga correspond to C1-2, and Ta corresponds to C1-3. Regarding Cd in C1-2, Wang et al. (2012) recently reported that there were two separate areas with high soil Cd contents: the city center and the north-west quadrant. Because the elements in C1 were shown to be associated with soil and during the sampling period Beijing experienced W, NW, and N airflows, airborne Cd levels were higher in the city's west and east than in the center, where it was diluted by moving air masses. The distribution of C1-2 also applied to C7 (Dy) and C9 (Zn), and C1-3 to C4 (W), C8 (Ba), and C10 (Pb). Wang et al. (2007) observed that Ba from fireworks in Beijing was 82 times higher than on 'normal' days. During the study period, fireworks were popular in Beijing due to The Spring Festival. This tradition increased Ba levels greatly; in addition, we can conclude that the southwest of Beijing set off the most firecrackers at that time. However, C2 (Cu and Bi), C3 (Mo), C5 (Ni), and C6 (Cr) had high values in the center of Beijing. Mo is an essential element for plants and exists widely in the following minerals: molybdenite, wulfenite, ferrimolybdate, jordisite, and powellite (Xu et al., 2013; Jiang et al., 2015a,b). Due to Mo's uptake and phloem mobility in plant roots, highly Mo-efficient plants can take up much Mo.³⁵ Thus, absorption of Mo by plants decreases airborne Mo levels, which may explain the lower content along the city's edge. Additionally, 80% of the Mo in China is used in steel-making, and there are still steel agencies and factories in the center of Beijing, which is likely the reason for the high Mo in the center.

Next, land cover data (for Beijing's main area) were used to analyze the local sources in detail. Fig. 4 shows the land cover and land use for Beijing's main district and the results of the profile analysis. The main zone is categorized into eight classes: farm land,

mixed forest, broad-leaved forest, coniferous forest, grassland, wetland, water, and artificial cover. In particular, the city center within the Fifth Ring Road is covered with artificial land; vegetation occupies almost the whole periphery of the city. The choice of the profile lines is based on the diversity of Beijing's surface. Thus, the trend was determined to go through from the northwest and southwest corners to the center. There is vegetation, artificial land, and water there. The profile analyses for C2, C4, and C7 are described in Fig. 4 because the three clusters are good examples. C2 (Cu and Bi), C3 (Mo), C5 (Ni), and C6 (Cr) were higher for artificial land; in contrast, C1-1 (Sm, Ho, Tb, Er, Yb, La, Lu, Th, Eu, Ce, Nd, Pr, Gd, and U), C1-2 (Cd, Co, Cs, Li, and Ga), C7 (Dy), and C9 (Zn) were higher for vegetation, and C1-3 (Ta), C4 (W), C8 (Ba), and C10 (Pb) had high values in the city center and the west. Because there is little water in the study area, the water type is not discussed, and Cd, Ba, and Mo were discussed above. As shown by previous studies, anthropogenic areas, like steel factories, road networks, and power plants, cause increased levels of certain elements in the air. Thus, these special land uses were also added to Fig. 4 to explore their relationship with certain elements. Song et al. (2012) analyzed the chemical characteristics of particulate matter in Beijing and reported that Cu was significantly correlated with vehicle emissions. In Fig. 4, the dense traffic areas lie in the city center and the southwest quadrant, where high Cu and Bi contents were found. Rodríguez Martín et al. (2015) showed that high concentrations of Ni were present in fly ash from coal-burning power plants and from atmospheric deposits and that the Cr anomaly was related to industrial pollution. During the study period, Ni contents were high in the center and northwest corner, where six power plants are located. Wang et al. (2012) also found that in Beijing, there was an "individual hotspot" of Cr in the south-east corner, where there was a factory; while in this study, a high zone of dustfall Cr was located

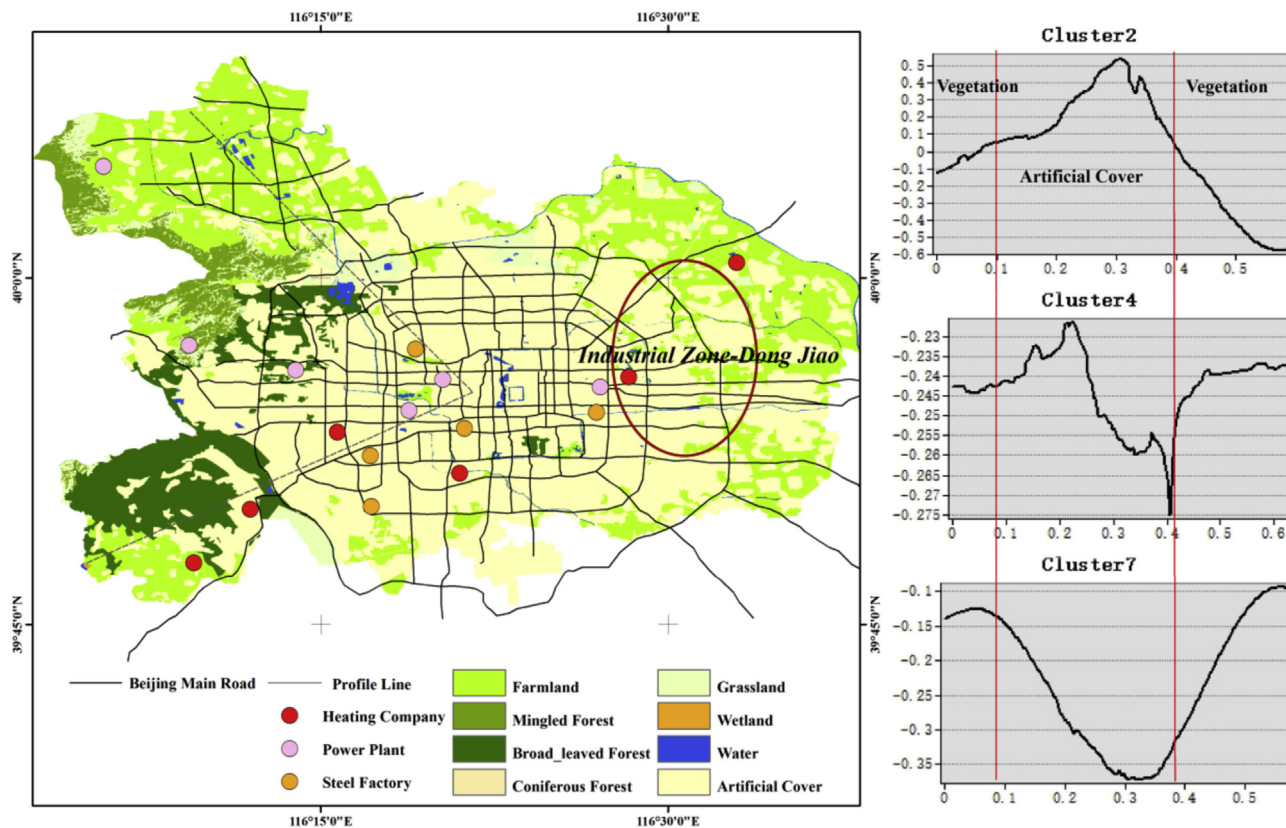


Fig. 4. Mapping of Beijing surface and results of profile analysis (The left is land cover and land use for Beijing main district. The surface is classified into 8 classes, namely farmland, mingled forest, broad-leaved forest, coniferous forest, grassland, wetland, water and artificial cover. The right is the profile analysis for cluster2, cluster 4 and cluster7. The profile trend is also shown as the left figure which goes through the northwest and southwest corners of the city to the center. It experiences the vegetation and artificial cover.).

to the east of the center of Beijing, which is the industrial district of Dong Jiao.

Also, the dustfall samples were collected in winter, so residential heating undoubtedly influenced the airborne elements. Yang et al. (2015) found a strong correlation with Zn and Pb, which are strong marker elements for coal combustion. However, in this study there was a significant difference in their distribution (See Fig. S6, Supplementary data): Zn levels were higher in the southwest and northeast corners of Beijing, while high Pb levels were found in the west and southeast quadrants of the city. This may be linked to Beijing's heating methods. Obviously, there are six heating companies located in the high Zn zone, suggesting that the heating companies may increase Zn levels. In turn, Pb levels may be aggravated by residential heaters. Pb has been found to be emitted mainly from automobile exhausts (Wang et al., 2001). However, it has to be noted that Beijing has restricted the use of leaded gasoline since 1998 and other fuels have the lead content limited to less than 0.013 gL^{-1} , so vehicle emissions are no longer a major source of Pb (Wu et al., 2011).

Finally, interpolated PCA was assigned to the main trajectories to quantify element immigration (Equation (1)). Here, only specific sites with high values were examined, and the ratios of IA and PCA were calculated and mapped (Fig. S7) to measure the contribution of remote sources to local element levels. The ratios were also analyzed with a Beijing DEM, which was grouped into two levels: low terrain (lower than 49 m) and high terrain (between 49 and 1175 m). For C4, C6, C7, C8, and C9, the ratios of IA and PCA were close to 0 or lower than 0.5 at all sites, indicating that remote pollutants contributed little to certain elements (W, Cr, Dy, Ba and Zn), while the ratios for C1-3, C2, and C3 were more than 0.5 at all

sites, signifying that Ta, Cu, Bi, and Mo were generated mainly by remote sources. Similarly, the values for C1-1, C1-2, and C5 were higher than 0.5, but only in the west in areas with high elevation, indicating that the transportation of the given elements from nearby cities in this zone was facilitated by the high terrain. For the remaining elements, no terrain influence was evident, possibly due to the larger effects of local sources. The value for C10 was higher than 0.7 in the east with low terrain, indicating that residential heating systems in nearby cities had a large influence on local Pb.

Study of major and trace elements extracted from the dustfall in Beijing and nearby cities can give direct information about the extent of airborne element pollution and provide a strong basis for the assessment of urban air quality. The challenge is to identify the element sources and to measure their relative contributions quantitatively. A statistical model integrating principal component analysis, correlation analysis, and cluster analysis was used to analyze the element data set. A geographic information system (GIS)-based approach with Kriging interpolation and backward trajectories with respect to different sites and elements was performed to quantify element immigration. In addition, this study highlights the whole distribution of dustfall elements, not just at a few sites, and can therefore provide a more powerful resource for environmental research. Moreover, we assessed 40 major and trace elements in the multielement analysis, which provided a more complete data set for source analysis.

4. Conclusion

This research concluded that industrial elements, like Cu, Mo, Ni, Cr, Ba, Zn and Pb, expose to human due to anthropogenic

activities; others, like rare earth element Li, Be, Ga, Pr, Nd, Sm, Eu, etc., enter into the environment through natural process. Specifically, high PCA scores are almost observed at industrial and residential areas such as power plants, steel factories and heating hotspots. Even some are located at suburban, agricultural, and rural sites with respect to given elements. In one word, 40 major and trace elements collected from Beijing dustfall have different sources and corresponding distributions. For example, high values of Zn and Pb that occur in winter have been suggested to be related with the use of heating system; and their distinct distributions are possibly due to various heating modes including personal or collective heating, heating fuels and heating facilities. Elevated values of Mo, Ni, Ba and Cu closely linked with intensive human activities have been demonstrated to originate from steel factories, power plants, firecrackers and automobile exhausts respectively. Rare earth elements, like Rb, Cs, Nb, Ta, Sc, Sr, La, Ce, etc., total 30 elements, have been indicated to be connected to the regional nature of urban surface soil. And more interestingly, the association of soil and dustfall collected from Beijing and nearby cities by 40 major and trace elements varies between sites. For instance the zone with the lowest correlation is located at the center of Beijing which is probably due to the heaviest traffic. Conversely, other areas have a higher relationship which implies that the nature of surface soil contributes a lot to the difference.

Subsequently, in order to study the effect of nearby cities on Beijing airborne elements, the air-mass patterns during the sampling period (15th Nov 2013 to 15th Mar 2014) in Beijing were analyzed: the airflow generated from the northwest quadrant to the city center contributed most to Beijing air flux, followed by the southeast air masses. Due to the small size of Beijing the air motion in winter was similar at each site; however, the spatial variation of PCA was evident partly due to the local emissions which can be further explained by terrain stretch. For example, the elemental transportation in C1-1, C1-2 and C3 from nearby cities in the west of Beijing is obviously facilitated by a high elevation. As for other elements, the terrain influence is not evident possibly due to the overriding of a larger local source. Then compared to other elements, the immigration factors of W, Cr and Dy are close to 0, and they are inferred to be totally influenced by the local emissions. The values of Ba, Zn and Pb are less than 0.5, which shows that they are partly governed by the local, too. However, Mo at certain sites has a high value more than 0.6, which indicates that Mo's deposition is mainly attributed to the regional transport.

In Summary, the study with respect to 40 major and trace elements collected from the dustfall in Beijing and nearby cities can give direct information about the levels of airborne elemental pollution and provide a strong basis for the assessment of urban air quality. In addition, this study highlights a whole distribution of the dustfall elements, not just a few sites, which can represent a more powerful tool to the environmental research; and it used 40 major and trace elements to do the multielement analysis, which can give a more scientific dataset to the source analysis.

Acknowledgment

This study was supported by the National Natural Science for Youth Foundation of China, under grant number 41201404. The authors gratefully acknowledge the NOAA Air Resources Laboratory for the HYSPLIT model. The authors are grateful to reviewers for important comments related to this paper.

Appendix A. Supplementary data

Supplementary data related to this article can be found at <http://dx.doi.org/10.1016/j.chemosphere.2016.02.099>.

References

- Ashbaugh, L.L., Malm, W.C., Sadeh, W.Z., 1985. A residence time probability analysis of sulfur concentrations at Grand-Canyon-National-Park. *Atmos. Environ.* 19, 1263–1270.
- Beddows, D.C.S., Dall, O.M., Harrison, R.M., 2009. Cluster analysis of rural, urban and curbside atmospheric particle size data. *Environ. Sci. Technol.* 43, 4694–4700.
- Beddows, D.C.S., Dall'Osto, M., Harrison, R.M., Kulmala, M., Asmi, A., Wiedensohler, A., Laj, P., Fjaeraa, A.M., Sellegri, K., Birmili, W., Bukowiecki, N., Weingartner, E., Baltensperger, U., Zdimal, V., Zikova, N., Putaud, J.P., Marinoni, A., Tunved, P., Hansson, H.C., Fiebig, M., Kivekäs, N., Swietlicki, E., Lihavainen, H., Asmi, E., Ulevicius, V., Aalto, P.P., Mihalopoulos, N., Kalivitis, N., Kalapov, I., Kiss, G., Leeuw, G.D., Henzing, B., O'Dowd, C., Jennings, S.G., Flentje, H., Meinhardt, F., Ries, L., Denier van der Gon, H.A.C., Visschedijk, A.J.H., 2014. Variations in tropospheric submicron particle size distributions across the European continent 2008–2009. *Atmos. Chem. Phys.* 14, 4327–4348.
- Biegalski, S.R., Hopke, P.K., 2004. Total potential source contribution function analysis of trace elements determined in aerosol samples collected near Lake Huron. *Environ. Sci. Technol.* 38, 4276–4284.
- Cao, Z.G., Yang, Y.H., Lu, J.L., Zhang, C.X., 2011. Atmospheric particle characterization, distribution, and deposition in Xi'an, Shaanxi Province, Central China. *Environ. Pollut.* 159, 577–584.
- Cape, J.N., Methven, J., Hudson, L.E., 2000. The use of trajectory cluster analysis to interpret trace gas measurements at Mace Head, Ireland. *Atmos. Environ.* 34, 3651–3663.
- Celo, V., Dabek-Zlotorzynska, E., McCurdy, M., 2015. Chemical characterization of exhaust emissions from selected Canadian Marine vessels: the case of trace metals and lanthanoids. *Environ. Sci. Technol.* 49, 5220–5226.
- Censi, P., Zuddas, P., Randazzo, L.A., Tamburo, E., Speziale, S., Cuttitta, A., Punturo, R., Arico, P., Santagata, R., 2011. Source and nature of inhaled atmospheric dust from trace element analyses of human bronchial fluids. *Environ. Sci. Technol.* 45, 6262–6267.
- Chen, W.T., Lu, S.H., Shao, M., Wang, M., Zeng, L.M., Yuan, B., Liu, Y., 2014a. Understanding primary and secondary sources of ambient carbonyl compounds in Beijing using the PMF model. *Atmos. Chem. Phys.* 14, 3047–3062.
- Chen, W.T., Shao, M., Lu, S.H., Wang, M., Zeng, L.M., Yuan, B., Liu, Y., 2014b. Understanding primary and secondary sources of ambient carbonyl compounds in Beijing using the PMF model. *Atmos. Chem. Phys.* 14, 3047–3062.
- Gaita, S.M., Boman, J., Gatari, M.J., Pettersson, J.B.C., Janhäll, S., 2014. Source apportionment and seasonal variation of PM_{2.5} in a Sub-Saharan African city: Nairobi, Kenya. *Atmos. Chem. Phys.* 14, 9977–9991.
- Gao, J.J., Tian, H.Z., Cheng, K., Lu, L., Wang, Y.X., Wu, Y., Zhu, C.Y., Liu, K.Y., Zhou, J.R., Liu, X.G., Chen, J., Hao, J.M., 2014. Seasonal and spatial variation of trace elements in multi-size airborne particulate matters of Beijing, China: mass concentration, enrichment characteristics, source apportionment, chemical speciation and bioavailability. *Atmos. Environ.* 99, 257–265.
- Green, L.C., Armstrong, S.R., 2003. Particulate matter in ambient air and mortality: toxicologic perspectives. *Regul. Toxicol. Pharm.* 38, 326–335.
- Jeong, C., Herod, D., Zlotorzynska, E.D., Ding, L., McGuire, M.L., Evans, G., 2013. Identification of the sources and geographic origins of black carbon using factor analysis at paired rural and urban sites. *Environ. Sci. Technol.* 47, 8462–8470.
- Jiang, Q., Sun, Y.L., Wang, Z., Yin, Y., 2015a. Aerosol composition and sources during the Chinese Spring Festival: fireworks, secondary aerosol, and holiday effects. *Atmos. Chem. Phys.* 15, 6023–6034.
- Jiang, W., Yang, Z.F., Yu, T., Hou, Q.Y., Zhong, C., Zheng, G.D., Yang, Z.Q., Li, J., 2015b. Evaluation of the potential effects of soil properties on molybdenum availability in soil and its risk estimation in paddy rice. *J. Soils. Sediments* 15, 1520–1530.
- Kim, S.Y., Yi, S.J., Eum, Y.S., Choi, H.J., Shin, H., Ryou, H.G., Kim, H., 2014. Ordinary kriging approach to predicting long-term particulate matter concentrations in seven major Korean cities. *Environ. Health Toxicol.* 29.
- Kitto, M.E., Anderson, D.L., Gordon, G.E., 1992. Olmen, I. Rare earth distributions in catalysts and airborne particles. *Environ. Sci. Technol.* 26, 1368–1375.
- Kleiman, G., Kheirbek, I., Graham, J., 2006. Appendix A: Application of Trajectory Analysis Methods to Sulfate Source Attribution Studies in the Northeast U.S. Appendix A: Trajectory Analysis Methods. A, pp. 1–15.
- Lin, Y.-C., Tsai, C.-J., Wu, Y.-C., Zhang, R., Chi, K.-H., Huang, Y.-T., Lin, S.-H., Hsu, S.-C., 2015. Characteristics of trace metals in traffic-derived particles in Hsuehshan Tunnel, Taiwan: size distribution, potential source, and fingerprinting metal ratio. *Atmos. Chem. Phys.* 15, 4117–4130.
- Olmez, L., Gordon, G.E., 1985. Reports: rare earths: atmospheric signatures for oil fired power plants and refineries. *Science* 229, 966–968.
- Pinxteren, D.V., Brüggemann, E., Gnauk, T., Müller, K., Thiel, C., Herrmann, H., 2010. A GIS based approach to back trajectory analysis for the source apportionment of aerosol constituents and its first application. *J. Atmos. Chem.* 67, 1–28.
- Qian, Z., He, Q., Lin, H.M., Kong, L., Liao, D., Dan, J., Bentley, C.M., Wang, B., 2007. Association of daily cause-specific mortality with ambient particle air pollution in Wuhan, China. *Environ. Res.* 105, 380–389.
- Reimann, C., Caritat, P.D., 2000. Intrinsic flaws of element enrichment factors (EFs) in environmental geochemistry. *Environ. Sci. Technol.* 34, 5084–5091.
- Robinson, N.H., Newton, H.M., Allan, J.D., Irwin, M., Hamilton, J.F., Flynn, M., Bower, K.N., Williams, P.I., Mills, G., Reeves, C.E., McFiggans, G., Coe, H., 2011. Source attribution of Bornean air masses by back trajectory analysis during the OP3 project. *Atmos. Chem. Phys.* 11, 9605–9630.
- Rodríguez Martín, J.A., Arana, C.D., Ramos-Miras, J.J., Gil, C., Boluda, R., 2015. Impact

- of 70 years urban growth associated with heavy metal pollution. *Environ. Pollut.* 196, 156–163.
- Shaltout, A.A., Khoder, M.I., El-Absawy, A.A., Hassan, S.K., Borges, D.L.G., 2013. Determination of rare earth elements in dust deposited on tree leaves from Greater Cairo using inductively coupled plasma mass spectrometry. *Environ. Pollut.* 178, 197–201.
- Shparyk, Y.S., Parpan, V.I., 2004. Heavy metal pollution and forest health in the Ukrainian Carpathians. *Environ. Pollut.* 130, 55–63.
- Song, S.J., Wu, Y., Jiang, J.K., Yang, L., Cheng, Y., Hao, J.M., 2012. Chemical characteristics of size-resolved PM_{2.5} at a roadside environment in Beijing, China. *Environ. Pollut.* 161, 215–221.
- Tan, J., Duan, J., Ma, Y., Yang, F., Cheng, Y., He, K., Yu, Y., Wang, J., 2014. Source of atmospheric heavy metals in winter in Foshan, China. *Sci. Total Environ.* 493, 262–270.
- Tang, Y., Han, G., Wu, Q.X., Xu, Z.F., 2013. Use of rare earth element patterns to trace the provenance of the atmospheric dust near Beijing, China. *Environ. Earth Sci.* 68, 871–879.
- Taylor, S.R., McLennan, S.M., 1995. The geochemical evolution of the continental crust. *Rev. Geophys.* 2, 241–265.
- Tian, H., Liu, K., Zhou, J., Lu, L., Hao, J., Qiu, P., Gao, J., Zhu, C., Wang, K., Hua, S., 2014. Atmospheric emission inventory of hazardous trace elements from China's coal-fired power plants temporal trends and spatial variation characteristics. *Environ. Sci. Technol.* 48, 3575–3582.
- Wang, C.X., Zhu, W., Peng, A., Guichreit, R., 2001. Comparative studies on the concentration of rare earth elements and heavy metals in the atmospheric particulate matter in Beijing, China, and in Delft, the Netherlands. *Environ. Int.* 26, 309–313.
- Wang, G.H., Cheng, C.L., Huang, Y., Tao, J., Ren, Y.Q., Wu, F., Meng, J.J., Li, J.J., Cheng, Y.T., Cao, J.J., Liu, S.X., Zhang, T., Zhang, R., Chen, Y.B., 2014. Evolution of aerosol chemistry in Xi'an, inland China, during the dust storm period of 2013 – Part 1: sources, chemical forms and formation mechanisms of nitrate and sulfate. *Atmos. Chem. Phys.* 14, 11571–11585.
- Wang, M., Bai, Y.Y., Chen, W.P., Markert, B., Peng, C., Ouyang, Z., 2012. A GIS technology based potential eco-risk assessment of metals in urban soils in Beijing, China. *Environ. Pollut.* 161, 235–242.
- Wang, Y., Zhuang, G., Xu, C., An, Z., 2007. The air pollution caused by the burning of fireworks during the lantern festival in Beijing. *Atmos. Environ.* 41, 417–431.
- Wang, Y.Q., Zhang, X.Y., Draxler, R.R., 2009. TrajStat: GIS-based software that uses various trajectory statistical analysis methods to identify potential sources from long-term air pollution measurement data. *Environ. Modell. Softw.* 24, 938–939.
- Wu, Y., Wang, R.J., Zhou, Y., Lin, B.H., Fu, L.X., He, K.B., Hao, J.M., 2011. On-road vehicle emission control in Beijing: past, present, and future. *Environ. Sci. Technol.* 45, 147–153.
- Xu, N., Braidia, W., Christodoulatos, C., Chen, J., 2013. A Review of molybdenum adsorption in soils/bed sediments: speciation, mechanism, and model applications. *Soil. Sediment. Contam.* 22, 912–929.
- Yang, J., Fu, Q., Guo, X.S., Chu, B.L., Yao, Y.W., Teng, Y.G., Wang, Y.Y., 2015. Concentrations and seasonal variation of ambient PM_{2.5} and associated metals at a typical residential area in Beijing, China. *Bull. Environ. Contam. Toxicol.* 94, 232–239.
- Zencak, Z., Klanova, J., H, Ivan, G, Orjan, 2007. Source apportionment of atmospheric PAHs in the western Balkans by natural abundance radiocarbon analysis. *Environ. Sci. Technol.* 41, 3850–3855.
- Zhang, J.P., Zhang, Q.H., Li, C.C., Shu, H.L., Ying, Y., Dai, Z.P., Wang, X., Liu, X.Y., Liang, A.M., Shen, H.X., Yi, B.Q., 2012. The impact of circulation patterns on regional transport pathways and air quality over Beijing and its surroundings. *Atmos. Chem. Phys.* 12, 5031–5053.
- Zhang, L., Wang, S.X., Wang, L., Hao, J.M., 2013. Atmospheric mercury concentration and chemical speciation at a rural site in Beijing, China: implications of mercury emission sources. *Atmos. Chem. Phys.* 13, 10505–10516.
- Zhang, R., Wang, H., Qian, Y., Rasch, P.J., Easter, R.C., Ma, P.-L., Singh, B., Huang, J., Fu, Q., 2015. Quantifying sources, transport, deposition, and radiative forcing of black carbon over the Himalayas and Tibetan Plateau. *Atmos. Chem. Phys.* 15, 6205–6223.